Organic & Biomolecular Chemistry

www.rsc.org/obc

Volume 6 | Number 14 | 21 July 2008 | Pages 2445–2640

ISSN 1477-0520

RSC Publishing

Bright molecules with sense, logic, numeracy and utility

A. Prasanna de Silva,* Thomas P. Vance, Matthew E. S. West and Glenn D. Wright

Received 20th February 2008
First published as an Advance Article on the web 2nd May 2008
DOI: 10.1039/b802963f

Using cartoons as an organizational aid, we illustrate how the 'fluorophore–spacer–receptor' format of fluorescent PET (photoinduced electron transfer) sensors and switches can be logically extended in many different directions. These include emissive sensors for various chemical species and properties, and exploit various kinds of emission. Common sensing issues such as dynamic range, internal referencing, selectivity, mapping and space resolution are addressed. The sensory output function is also developed into more complex forms, molecular logic/computation being one such example. Molecular logic leads to molecular arithmetic. Real-life applications to physiological monitoring, medical diagnostics and molecular computational identification of small objects are included.

1. Introduction

We humans pride ourselves on being able to apply logic in our dealings. Our economies would be far less sophisticated if numbers did not underpin them. We (as well as other life-forms) depend on several senses, such as vision, for our survival and success. Most of us also like to be useful to the rest of society. Amazingly, these valued features of sense, logic, numeracy and utility are also displayed—at least at a rudimentary level—by molecules built largely according to a single design. These molecules need to be bright, not because they accomplish functions often ascribed to some degree of intelligence, but because they need to emit light signals in order to communicate with their human handlers—us. These molecules can gather and process information from humanly significant spaces so small that only they have access. So their value to general society can be significant

In this perspective, we will outline the entry-level design and then show how it can be taken logically in many different directions—one of these directions even forming a new experimental field. Fig. 1 illustrates how directly these various avenues arise. Once a few conditions are met, each of these cartoons can generate many different chemical structures aimed towards various chemical situations. Examples will be chosen to set each of these cartoons in context.

School of Chemistry and Chemical Engineering, Queen's University, Belfast, BT9 5AG, Northern Ireland

2. Cartoon 1: the basic sensor/switch system

One of the early examples of a 'fluorophore–spacer–receptor' system[1] is our **1**.[2] Here, we set out to demonstrate an 'off–on' fluorescent sensor for Na^+ with a quantitatively rational design basis. The excited state energy of the cyanoanthracene fluorophore is 3.0 eV.[3] Its reduction potential is −1.6 eV. The oxidation potential of the π-system in the benzo-15-crown-5 ether receptor is +1.4 eV. Thus the photoexcited state contains sufficient energy to drive an electron from the receptor to the fluorophore.[4] So the fluorescence capacity of **1** is ruined, even though the transferred electron is returned after a few picoseconds. **1**'s 'off state' is caused by photoinduced electron transfer (PET).[5–7] **1**'s relative photostability is ensured by thermal back electron transfer.

Glenn D. Wright, A. Prasanna de Silva, Thomas P. Vance and Matthew E. S. West

Raised in places as diverse as Colombo, Bangor, Enniskillen and Carrickfergus, the authors share the common factor of PhD study in organic photochemistry at Queen's University of Belfast, Northern Ireland. Generalization of the fluorescent PET sensor principle and the invention of molecular logic gates happened here. Rock-climbing, water-skiing, percussion and following local football keep the authors off the streets when out of the lab.

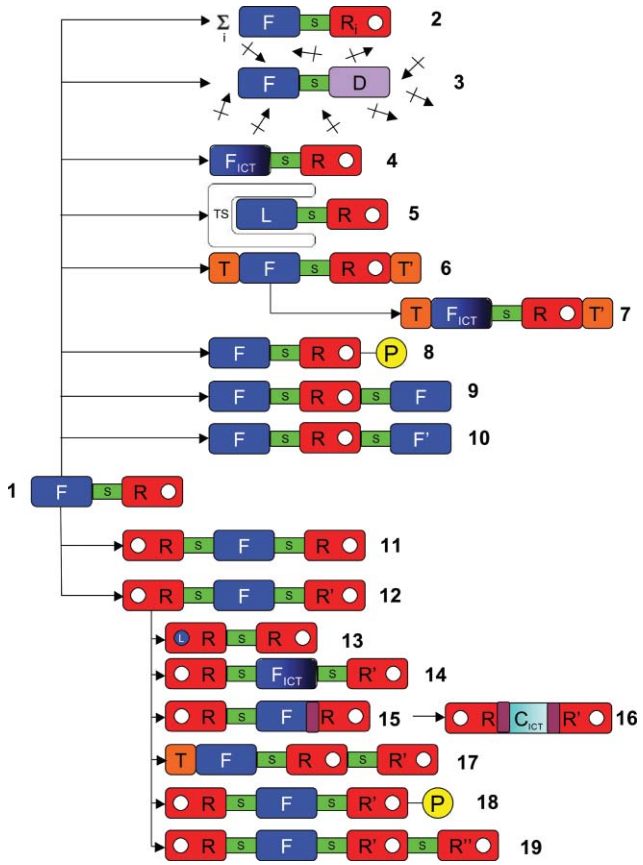

Fig. 1 Cartoons illustrating the logical extensions of the 'fluorophore–spacer–receptor' format of fluorescent PET (photoinduced electron transfer) sensors and switches. Legend: F (in blue) = fluorophore, S (in green) = spacer, R (in red) = receptor, D (in pale violet) = electron donor, F_{ICT} (in shaded blue) = fluorophore with an internal charge transfer (ICT) excited state, L (in blue) = lumophore, TS (in white) = transparent sheath, T (in orange) = targeting group, C_{ICT} (in shaded pale blue) = chromophore with an internal charge transfer (ICT) excited state, P (in yellow) = polymer, ⇝ = solvent dipole. Regions of overlap between fluorophores/chromophores and receptors are shown in violet.

How do we achieve **1**'s 'on' state? The entry of Na^+ into the suitably sized cavity of the benzo-15-crown-5 ether naturally increases the oxidation potential of the latter. So the photoexcited state is no longer able to drive the electron transfer to the fluorophore from the receptor (now Na^+-bound). From another point of view, the electric field of Na^+ holds the electron back. The eventual de-excitation of the photoexcited state (after a few nanoseconds) gives observable fluorescence.

Though structurally uncomplicated, **1** has excellent selectivity for signalling Na^+ in the presence of H^+ —which is exploited in Section 13. Discrimination among alkali cations is not great, but **1**'s progeny improves this aspect to the point of social impact and commercial success (Section 9). A mutation of **1**'s receptor module into a calixarene crown produces **2**,[8] which allows the selective monitoring of Cs^+ in 'hot' nuclear waste, which is both acidic and saline. Overall, hundreds of examples of 'fluorophore–spacer–receptor' systems are now available.[7,9] For instance, our **3**[10]—trademarked as lysosensor blue™—detects intracellular acidic compartments by emitting blue fluorescence.[11] It helps radiologists to understand how γ-rays cause cell damage during radiotherapy.[12] The H^+-driven switching efficiency of **3** in a chemical context is clearly visible in Fig. 2.

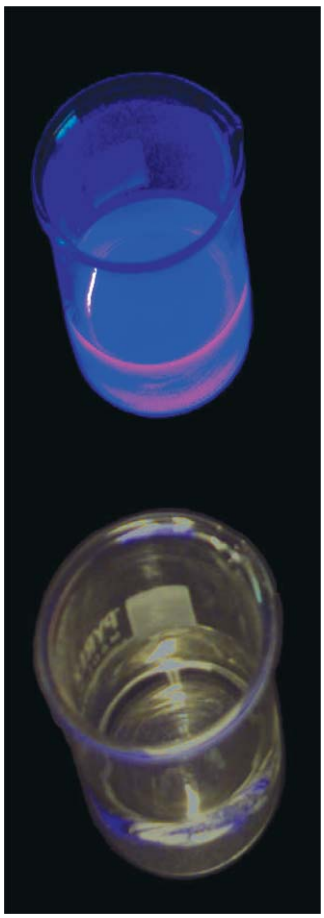

Fig. 2 Beakers containing a solution of **3** without (bottom) and with (top) addition of H^+ as a target, while under ultraviolet (366 nm) irradiation.

3. Cartoon 2: sensor systems with wide dynamic range

Cartoon 1 illustrated how covalent linking of a receptor (for chemical transactions) *via* a spacer produced an autonomous intelligence-gathering molecule. Such an autonomous system *e.g.* **3**, can function without losing integrity in multicompartmental biological environments.[13] However, covalent linking can be given up to gain other advantages, as done in the case of producing sensing ensembles.[14,15] We now wish to gain the advantage of a very wide dynamic range of sensory action.[16] Molecular sensors only show a good response over a narrow range of analyte concentrations, as illustrated by the famous 2 pH unit indicator range.[17] Eqn (1) describes this response function.[18]

$$\log[(I_{Fmax} - I_F)/(I_F - I_{Fmin})] = -pH + pK_a \quad (1)$$

So we use a simple mixture of several 'fluorophore–spacer–receptor' systems **3–6** where everything remains the same except

for the various receptors, which are carefully chosen so that their pK_a values fit an arithmetic progression. This series can be predicted by numerically maximizing the linearity of the fluorescence intensity–pH response curve of the additive mixture as a function of the pK_a values. This means the sensing range of each 'fluorophore–spacer–receptor' system meshes with the others in the manner of an athletics relay team. When the action of one finishes, another takes over, and so on as we traverse the pH range.

4. Cartoon 3: sensors for polarity

What if a 'fluorophore–spacer–receptor' system lost its chemical reception ability? The conditions for PET can be maintained by conserving the essential π-system. For instance, the crown ether of **1** can be sawn off to produce **7**.[19] If the driving force for PET is not too large, such cases can be manipulated in a useful way. The redox potentials, which make up the PET driving force, are usually measured in polar organic aprotic media.[3] Therefore if we imagine PET in less polar media, the driving force becomes endergonic because the radical ion pair state is less solvated.[20] With PET thus weakened, fluorescence predominates as the de-excitation channel. So we have fluorescence switching 'on' in **7** as the solvent polarity is reduced.[19,21,22] Of course, this effect can ambush experiments that are aiming to measure chemical species in intracellular environments if we are not careful.

The H^+-driven fluorescence switching 'on' of **8**[23] can be predicted from older electrochemical data[24] and from previous closely-related fluorescent PET sensors.[25] So it is not surprising that protonation of **8** enhances the fluorescence quantum yield by a factor of 165 in aqueous methanol. However, attempting[23] to employ **8** as an intracellular pH probe is unsuccessful. Instead, **8** localizes in intracellular membrane structures of low polarity, where it then becomes strongly fluorescent in a pH-independent manner.

5. Cartoon 4: one-way PET

Cartoon 4 arises from cartoon 1 by a subtle mutation. The fluorophore, being based on an internal charge transfer (ICT) excited state,[7,26,27] presents a substantial electric field to its surroundings. Many push–pull π-systems with graded electron density are of this type.[28] Such a field can repel or attract inbound electrons from a receptor depending on its orientation. If the driving force for PET is exergonic but not too large, such an electric repulsion can stop the PET and fluorescence is switched 'on'. This is the case for **9**.[29] If the same fluorophore were attached to the 'fluorophore–spacer–receptor' with the opposite orientation (**10**), the electric attraction augments the driving force for PET and fluorescence is switched 'off'. Of course, the fluorescence of **10** can be switched 'on' by protonation of the amine receptor (as normally seen under cartoon 1). On the other hand, H^+-induced fluorescence switching of **9** is poor, since it is already rather fluorescent in the absence of H^+.[29]

The photogenerated electric field is only half the explanation for the clearly different photophysics displayed by the regioisomers **9** and **10**. Gao and Marcus' theoretical study showed that the imide nitrogen is a node in both frontier orbitals of both **9** and **10**.[30] Hence PET is more difficult across the imide nitrogen. The relative importance of these two explanations can be tested by mutating **9** and **10** into **11** and **12** respectively so that the direction of PET is reversed.[31] Pyridine receptors encourage PET towards them, once protonated.[32] The driving forces for PET for protonated **11** and **12** are close to zero, making them appropriate for the test. H^+-induced fluorescence switching is poor in both cases and most importantly, no significant regiochemical differences are seen. So both explanations turn out to be of equal importance.[31]

Qian *et al.* extend the structural landscape around these cases in two educational ways. Though PET is suppressed in **9**, there is an intramolecular hydrogen bond, albeit weak, between the protonated aliphatic amine and a carbonyl oxygen which noticeably reduces the fluorescence efficiency of protonated **9** by introducing a vibrational energy loss mechanism.[33] Qian *et al.*'s **13**[34] possesses an iminothiazolidine unit instead of the aliphatic amine of **9**. When protonated, the latter reduces its fluorescence strongly because the hydrogen bonding to the carbonyl oxygen is extensive. Their **14**[35] is also a structural adjustment of **9**, with the receptor a tertiary aromatic amine, which is more oxidizable than an aliphatic counterpart. This makes the driving force for PET from the receptor to the fluorophore significantly more exergonic (than that for **9**)—so exergonic that the photogenerated electric field and the node cannot stand in the way of the transferring electron. Normal PET service in the manner of cartoon 1 is resumed and **14** displays nice H^+-induced fluorescence switching 'on'. This case is remarkable because the receptor is a proton sponge (1,8-bis(dimethylamino)naphthalene) and therefore, is extremely efficient. The experimentally found pK_a value is 10.8. Although the receptor is not physically separated from the fluorophore by an alkyl spacer, electronic separation is the upshot.

6. Cartoon 5: phosphorescent sensors

The bulk of this perspective concerns emission from excited singlet states. Can excited triplet states contribute to the cause? Indeed, room temperature phosphorescence (RTP) is worth co-opting into 'lumophore–spacer–receptor' systems, because the millisecond lifetime of triplet states gives them an advantage. Signal detection becomes easier by time-gating out any background fluorescence lasting just nanoseconds. However, the triplet excited states of aromatic π-systems that gave rise to RTP are notorious in being killed off by the merest whiff of dioxygen. A nice way of minimizing this problem is to encase the triplet state in a transparent sheath[36,37] so that only photons can get in and out. In our present case however, we need to ensure that the 'normal' receptor R remains accessible to the analyte. Luckily, such regioselective encapsulation can be arranged by exploiting the hydrophobic forces between β-cyclodextrins and aromatic compounds in water. **15**[38] was the first case, while **16**[39] and **17**[40] are more recent incarnations. Obviously the driving force for PET in these cases must be evaluated for the triplet excited state.[41]

7. Cartoon 6: membrane-targeted sensors

The value in accessing small spaces with molecular spies was indicated in the introduction. We need to outfit the molecules with suitable vehicles to take them there. Targeting modules of controlled hydrophobicity, as measured by Hansch *et al.*,[42] can serve this purpose in simpler situations. These would target each of the molecular spies to a location of matching hydrophobicity, thereby allowing us to build up a picture of the distribution of an analyte in a field. Cartoon 6 has a main targeting module T

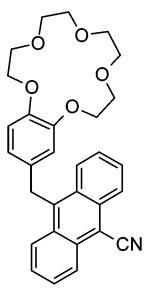

1

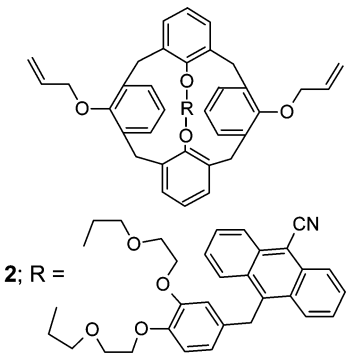

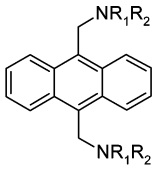

3; $R_1 = R_2 = Et$
4; $R_1 = R_2 = CH_2CH_2OH$
5; $R_1 = H$, $R_2 = CH_2CH_2NEt_2$
6; R_1, $R_2 = CH_2CH_2N(Me)CH_2CH_2$

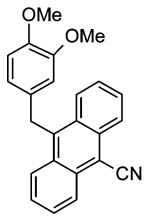

7

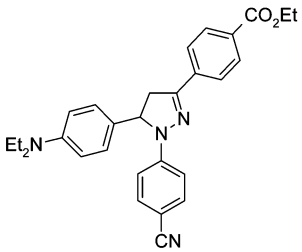

8

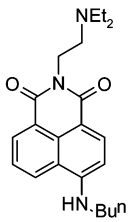

9

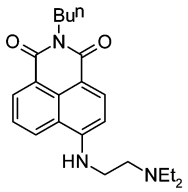

10

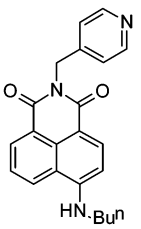

11

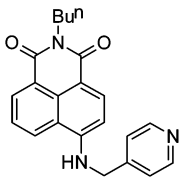

12

for gross positioning and another targeting module T' for fine-tuning of the receptor location to where the analyte information is to be gathered. H^+-sensing **18**[43] is one of a family in which all members localize in detergent micelles dispersed in water. Each family member takes up residence at the nanoscopic position that is suited to the hydrophobicity of its receptor module. Indeed, the local effective H^+ density (as measured by the deviation of the operational pK_a value seen in water for suitable model compounds) is found to be a smooth function of T' hydrophobicity. Such functions can shed light on the Gouy–Chapman region near the micelle surface. After all, H^+ densities near biomembranes are responsible for energy generation for all the subsequent activities of cells.[44]

Nakahara *et al.*'s **19** is a particularly successful example of a micelle-targeted PET system that achieves the selective measurement of Ba^{2+}.[45] The reduced polarity of the neutral micelle environment cuts down **19**'s effective basicity so that some degree of Ba^{2+} measurement can be carried out at a reasonable pH value. In neat aqueous solution, little fluorescence enhancement is observed due to the poor complexation of **19** with Ba^{2+}.

8. Cartoon 7: sensors for mapping membrane-bound species

Adding in aspects of cartoon 4 gives us a way of seriously improving our ambition concerning cartoon 6. Mapping ion densities in nanospaces near membranes would be so useful. However, any map requires a method of estimating position. How do we estimate positions in daily life? We define positions by referencing them to landmarks nearby. We can do something similar with molecular spies by asking, what polarity do you sense in your immediate environment? Fluorophores with ICT excited states show smooth red shifts in their fluorescence wavelengths in response to a rising in polarity of their environments.

The answer to the above question would be an estimate of position in situations where a radial coordinate is a satisfactory descriptor. Detergent micelles of a spherical nature in water would fit the bill. Of course, the PET design of cartoon 7 allows the measurement of the local effective concentration of a chosen analyte. Now we have a local analyte level for a known position. Different data-pairs like this, obtained from various molecular

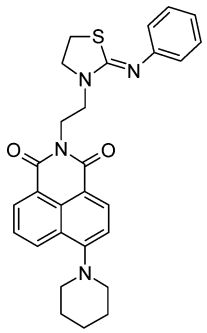

13

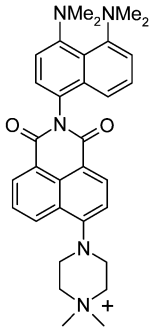

14

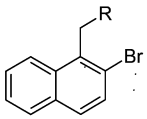

15; R = NEt_2

16; R = $N(CH_2CH_2OH)_2$

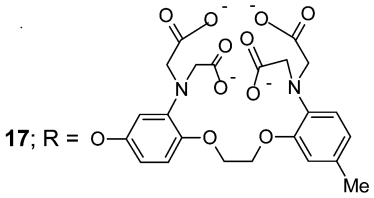

17; R =

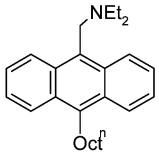

18

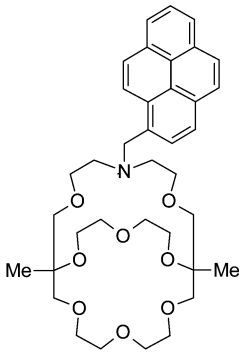

19

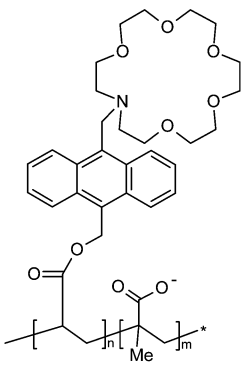

20

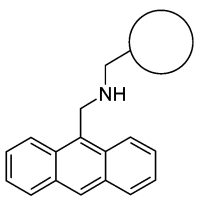

21

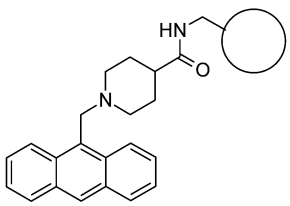

22

spies hydrophobically targeted to a range of positions in micellar media, lead to lovely maps.[46]

9. Cartoon 8: polymer-bound sensors/switches

The very act of connecting a 'fluorophore–spacer–receptor' system by either end to a polymer species, creates a larger space-scale where our molecular spy becomes a small but active component. Such a situation is exploitable in different ways.

If the polymer is water-soluble but organic in nature, we are almost back to the situation in Section 7. In spite of its linkage, the molecular spy is able to select its nanoenvironment within the polymer coils and then measure suitable analytes at that location. Klok and Moller's **20** is an early, but visionary, effort in this direction,[47] based on one of the earliest spy components.[48] The anionic nature of the polymer electrostatically concentrates K^+ so that the detection sensitivity of the molecular spy is enhanced.

If the polymer is suitably cross-linked so as to be insoluble, we can have objects that are large enough to be observable by the naked eye. Being able to see these gives them an extra sense of validity and also allows them to be manipulated with confidence.[49] Such manipulations include recovery for re-use. Of course, the downside is that the sub-nanometric spatial resolution of our molecular spy is sacrificed. The first PET system of this kind, **21**, arising from Soumillion in collaboration with us,[50] was one where silica was the polymer and H^+ the analyte. Miller and Copeland's more recent **22**, based on an organic polymer gel bead, allows the screening of bead-bound catalysts for local H^+ generation from substrates in solution.[51]

In Section 2, we promised examples of social and commercial value. Here they are: Roche's Tusa and He, in collaboration with us, designed **23**, **24** and **25** as sensors for Na^+, K^+ and Ca^{2+} respectively in whole untreated blood.[52] These cases are connected to an organic polymer fibre mat. Red blood cells are held back by

this mat and only the nearly colourless serum passes through to be illuminated. The fluorescence intensity that results is directly related to the concentration of the appropriate blood electrolyte. **23**, **24** and **25** are part of a blood chemistry module (Fig. 3) which is very widely used in hospital critical care units, ambulances, general practice offices and even in veterinary settings.[53] A conservative estimate of sales of this blood chemistry module is US$50 million so far.

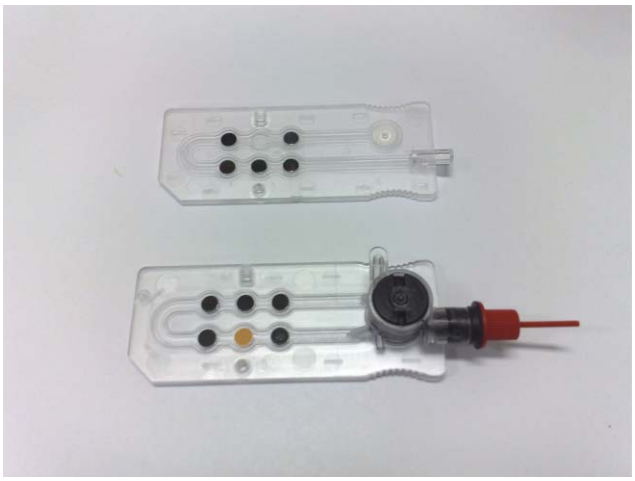

Fig. 3 OPTI LION® (top) and OPTI R® (bottom) cassettes sold by Optimedical Inc. (www.optimedical.com). The black spots carry the organic polymer fibre mats with the appropriate sensor molecules covalently attached. Na^+, K^+, Ca^{2+}, pH and CO_2 are measured by the fluorescence of these spots. The orange spot in the bottom example is similar and responds to dioxygen.

A small, active component on a much larger object can perform other valuable functions. Take a face, for instance. We recognize an approaching friend by subconsciously asking, and obtaining answers for, a myriad of questions about his or her face. So we can employ our small, active component as a means of identifying objects as small as *ca.* 100 nm by asking questions like: 'what's the excitation wavelength?', 'what's the emission wavelength?' and 'what's the fluorescence intensity response to various analytes?'. Cartoon 8 can be combined with other situations to allow the issuing of individual identities to rather large populations of small micrometric objects, which current technologies struggle to do. This will be developed in Section 19.

10. Cartoon 9: statistically enhanced PET

'Strength in numbers'—what can this old adage contribute to 'fluorophore–spacer–receptor' systems? The introduction of an extra fluorophore (and spacer) is considered in cartoon 9. Another permutation of modules is also possible in this scenario. Optical excitation at non-laser intensities will only excite one fluorophore, but energy migration can occur between the two F units. Thus the PET process from the receptor can occur to either fluorophore, *i.e.* a statistical enhancement of the PET process can be seen. Comparison of bifluorophoric **26** with its monofluorophoric sibling **27** appears to bear out this expectation.[54] Related, but larger, PET enhancements are seen in conjugated polymers when they interact with other species because the exciton can delocalize over considerable distances.[55]

11. Cartoon 10: internally referenced sensors

The bifluorophoric case, where two different fluorophores are used, allows the design of PET to occur to F, but not to F'. What use is this? The PET-inactive fluorophore serves as an innocent bystander while the PET-active fluorophore's emission responds to the analyte. So we have a two-colour output where one channel is analyte-dependant while the other serves as an internal reference. Internal references are excellent for calibrating the analytical signal against vagaries such as unknown optical path-length and unknown sensor concentration (due to various degrees and types of sensor decomposition, as well as unknown degrees of sensor incorporation). It is no wonder that such ratiometry is popular in intracellular studies, especially with integrated 'fluorophore–receptor' systems with ICT excited states.[13] Bifluorophoric molecules need careful design to allow the reasonable optical excitation of either fluorophore at will. Serendipity is needed to keep the electronic energy transfer (EET) (which can drain the higher energy fluorophore) within reasonable bounds. It is gratifying therefore that **28** proves the principles rather nicely[56] and that Samanta and Banthia's **29** carries on the effort[57] along this line of research.

12. Cartoon 11: geometry-selective sensors

What benefits, if any, can be gained by employing two receptors as shown in cartoon 11? There is, of course, the statistical advantage[55] similar to that discussed in Section 10. With it comes a disadvantage in that fluorescence is only switched 'on' when the second receptor is guest-bound. When the guest is an ion, the approach of the guest to the second receptor is hindered by the repulsive electric field exerted by the guest already bound to the first receptor. So only rather high guest concentrations can cause the switching 'on' of fluorescence. This disadvantage has been cleverly converted into a lovely way of detecting protein phosphorylation[58] and even cell apoptosis.[59] **30** cannot bind the second Zn^{2+} under normally achievable concentrations until the repulsive field is mitigated by the negative charge of the phosphate group. The apoptosis sensor exploits the difference in charge between phosphatidyl choline (predominant in the outer leaflet of membranes in normal cells) and phosphatidyl serine (sent to the outer leaflet from the inner layer when the cell becomes apoptotic and is ready to die). These are shining examples of fluorescent PET sensing solutions to hard biological problems.

However, the first demonstrable benefit of cartoon 11 concerned geometry-selective fluorescent sensing. In the simplest case, this is length recognition and signalling. **31** selects the 'molecules of death' putrescine and cadaverine (α,ω-pentanediamine and -butanediamine) in their diprotonated forms.[60] Aspects of the chelate effect of inorganic chemistry[61] and the neighbouring group participation of physical organic chemistry[62] play a part in this success since the fluorescence of **31** is not switched 'on' by protonated methylamine until rather high concentrations are reached. It is only fair to note another length-selective fluorescent sensor of the same vintage,[63] though resting on a non-PET foundation. **32**[64] continues the good work by improving the selectivity of the fluorescent PET sensing of glucose seen in the monoreceptor version.

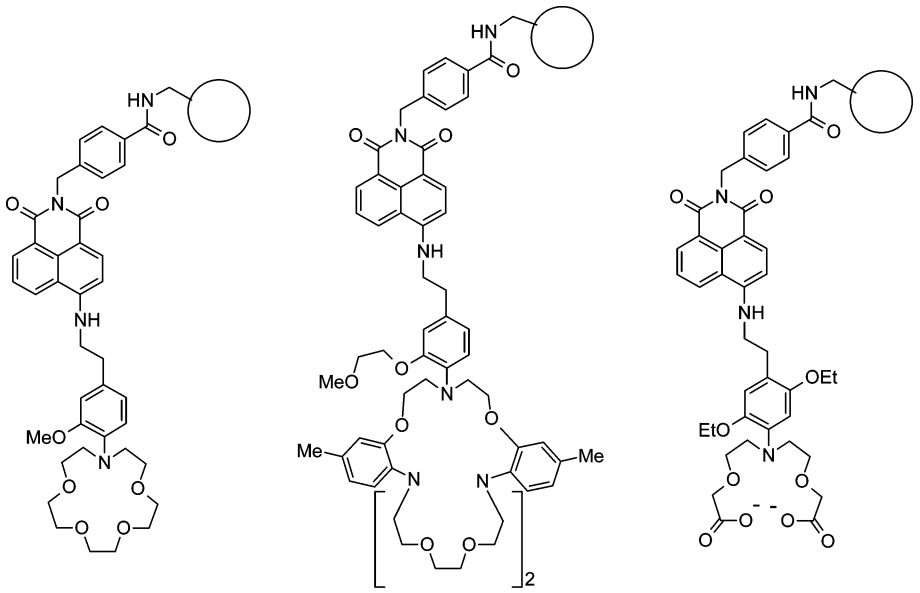

23 24 25

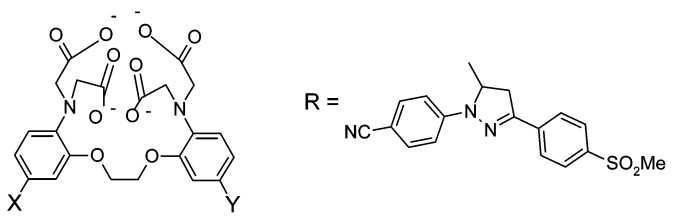

26; X = Y = R
27; X = Me, Y = R

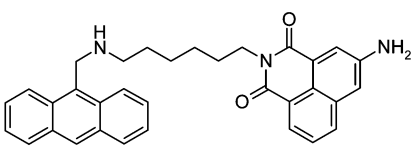

28

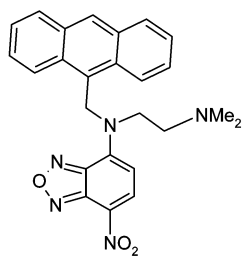

29

13. Cartoon 12: molecular logic and 'off–on–off' systems

The apparently small step of allowing the receptors to be non-identical, as seen in cartoon 12 and its possible permutations, allows us to enter a new area concerned with mathematics, physics and information engineering. In fact the experimental field of molecular logic and computation[65–68] was launched in this way with **33**.[69] Then and now, theoretical speculation and outright hype haunt this field. It is only experimental work, reproducible and extensible by laboratories worldwide, that will allow a sober assessment of what this field can realistically achieve. **33** has allowed this examination to begin in earnest. The following few paragraphs cannot do justice to the developments, but reviews and commentaries[65–68] can be consulted by the interested reader.

33 picks up H^+ by virtue of its amine receptor and gathers Na^+ because of its benzo-15-crown-5 ether unit. From a computing viewpoint, **33** is driven by H^+ and Na^+ inputs. Its output is fluorescence. Fluorescence only emerges when the PET capabilities of both receptors are blocked by the bound guests. Since fluorescence is switched 'on' only when H^+ and Na^+ are bound, **33** can be recognised as an AND logic gate according to the Boolean[70] definition.[71] Bharadwaj and Bag's **34** is a recent fluorescent PET-based AND gate driven by Zn^{2+} and Na^+ inputs targeting an aza-15-crown-5 ether and a cryptand respectively.[72] **34** is interesting among AND gates because of the large fluorescence enhancement produced.

AND is only one of many Boolean binary logic operations[71] that can now be emulated on the molecular-scale. For instance **1**,[2] which exemplified cartoon 1, represents a YES logic gate since a high level of fluorescence output emerges only when a high level of

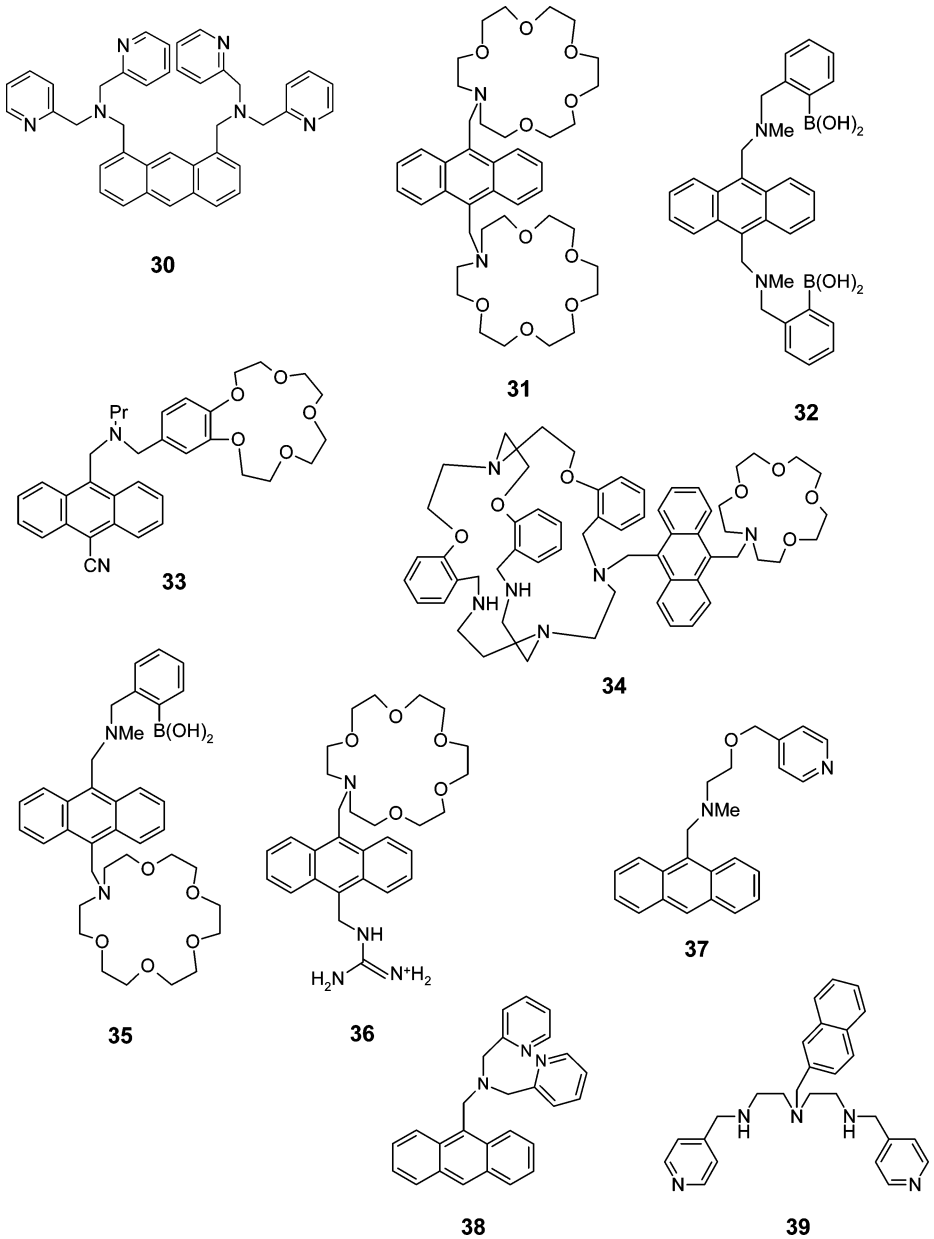

H^+ input is present. Also there are cases of cartoon 1 that can be rationally designed to produce PET only when a high level of H^+ is present so that fluorescence is effectively switched 'off'.[73] This corresponds to NOT logic. In fact, all the one-input and two-input logic types can be achieved in this or related ways.

Though fluorescent PET systems were the first approach to molecular logic and computation, nowadays they represent only one of many approaches.[65–68] Fluorescent EET systems involving DNA hybridization with or without enzyme action have also yielded numerous examples. Chemically responsive photochromic systems have also yielded a large crop. Natural enzymes, singly or in tandem, also provide a rich source. Even simpler colour-forming chemical reactions can, in ingenious hands,[74] be seen as rather complex logic gate arrays.

The AND logic gates of cartoon 12 can be adapted so that the two receptors receive two functionalities from the one guest, rather than capturing two unconnected guests as **33** does. Then, fluorescent sensors with excellent selectivity for bifunctional guests are produced. James and Cooper's **35** looks for a diol functionality and an ammonium group *via* its boronic acid and aza-18-crown-6 ether receptors. Naturally, the fluorescence of **35** switches 'on' only in the presence of protonated glucosamine but not glucose or protonated methylamine.[75] Our **36** is less efficient in targeting the brain neurotransmitter γ-amino butyric acid (GABA) since only one of its two receptors (the aza-18-crown-6 ether) is PET-active.[76]

Let's take ourselves away from molecular logic and computation for now, to another research direction that cartoon 12 (and its permutations) give birth to. What if the two receptors target the same guest, but with different binding strengths? Also, and importantly, the tighter-binding receptor is PET-active only when the guest is absent whereas the weaker-binding receptor becomes PET-active only when the guest is bound in it. Then, when the guest is H^+, an interesting type of fluorescence–pH profile arises. Such a bell-shaped profile has 'off–on–off' fluorescence action when

the pH is monotonically reduced. The survival of most species depends on environmental variables in this 'off–on–off' way. This is also the principle of the middle path prescribed in Buddhism for many human activities, since too much or too little of a good thing gets us in trouble. After the first cases, **37**[77] and **38**[78] based on a permutation of cartoon 12, newer examples such as Pina and Garcia-Espana *et al.*'s **39**[79] provide interesting extensions by combining Zn^{2+}-driven 'off–on' with H^+-driven 'off–on–off' action. Here the pH window signalled by 'on' fluorescence is narrowed considerably in the presence of Zn^{2+}, which is a nice discovery.

14. Cartoon 13: sensors based on lanthanide luminescence

Up to now, inorganic chemistry has been encountered in this article only tangentially, in terms of the metal ion coordination chemistry of the receptor modules. Now we meet inorganic chemistry full in the face, when the metal ion pops up in the form of the lumophore itself. In fact, the light emission signal is an inorganic signature. So the development of cartoon 13, as exemplified by **40**[80] and **41**,[81] was an important step in the generalization of the fluorescent PET sensor/switch principle. The lumophore metal ion is set in a selective receptor R' which is connected *via* a spacer to the 'normal' receptor R which targets the analyte (*e.g.* K^+ in the case of **41**). As is well-documented,[82–84] light energy needs to be passed to lanthanide metal ions like Tb^{3+} and Eu^{3+} *via* the much better absorbing aromatic receptor R' and subsequent EET.[7] The mechanistic situation is complicated since electron transfer, say, from receptor R can occur to the excited lanthanide centre or to the triplet excited state of aromatic receptor R'. Nevertheless, these sensing/switching systems have the advantage of operating smoothly in intrinsically fluorescent environments because the millisecond lifetime of lanthanide ion emission can be time-sliced away from the organic fluorescence in the nanosecond regime. This is just like the phosphorescent systems discussed in Section 6, but without their oxygen sensitivity. The aza-18-crown-6 ether receptors in **41** allow the targeting of K^+ whereas the amine receptors in **40** can only tackle H^+. The use of two R receptors in both these instances arose out of synthetic convenience. Sensors based on lanthanide luminescence have been taken forward by Parker[83] and Gunnlaugsson and Leonard[84] for instance.

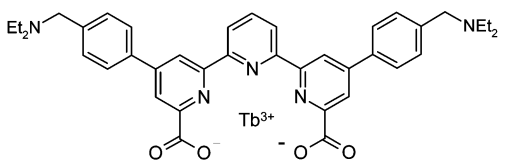

40

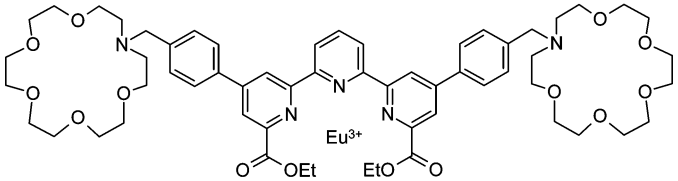

41

15. Cartoon 14: path-selective PET

Our discussion of **9** and **10** regarding cartoon 4 illustrated how important regiochemical influences were in determining the efficiency of some fluorescent PET switches. ICT excited states were involved in this effect. Conceptual combination of **9** and **10** produces **42** and **43**, representing cartoon 14.[85] Both receptors target H^+ but with measurably different binding strengths. PET only occurs from one receptor and not the other, even though the driving force for either is virtually the same. Actually, it's not the receptor that matters in this instance but the position on the ICT fluorophore to which it is attached. PET only occurs from the receptor attached to the 4-amino group of the 4-aminonaphthalimide fluorophore. A similar path-selective PET occurs in a much more important sphere: the photosynthetic reaction centre (PRC).[86] While picosecond laser spectroscopy is needed to conduct this experiment on the PRC, **42** and **43** can be analyzed with the far simpler technique of pH-dependent fluorescence. It is gratifying that the contribution of the electric field from the ICT excited state of **42** and **43** to their path-selective PET ties up nicely with suggestions of protein electric fields causing the effect within the PRC.[87]

16. Cartoon 15: three-state fluorescent switches

Until now, this article has employed spacer units between the photoactive and chemically active groups, which maintains the modularity of the latter. What if one of these spacers of cartoon 14 is excised? In fact, the removal of the spacer from cartoon 1 is instructive. This leads to integrated 'fluorophore–receptor' systems with ICT excited states, which underpin many early fluorescent pH indicators, including some that were brought back from the New World by Spanish explorers.[88,89] Some of their cousins have become very popular fluorescent sensors for intracellular species such as Ca^{2+}.[13] PET systems, which are the focus of this article, have a far shorter history, but their predictive design has led to widespread adoption and commercial success.[52] The complementary features of PET and integrated ICT systems[7] mean that one or the other approach can usually help with the problems facing the sensor community.

The excision of one spacer in cartoon 14 leads us to cartoon 15, which is an integration of an integrated 'fluorophore–receptor' system with a PET system. So we have a chance to marry the complementary features of these systems. **44** is an effort in this direction.[90] **44**'s fluorescence is switched 'on' at low pH but drops to a plateau of about half the original intensity as the morpholine receptor becomes free of H^+ at medium pH. The PET rate in this instance happens to compete equally with fluorescence for the deactivation of the excited state. At even higher pH, the NH group deprotonates, so that the N^- is the receptor R in cartoon 15. The π-system so-produced is virtually non-fluorescent, presumably *via* coupling of the ICT excited state to hydrogen bonded water oscillators.[33] So we have three clear states of fluorescence output at 'high', 'medium' and 'low' plateaux. Ternary logic can have interesting uses[91] and will be discussed in Section 19.

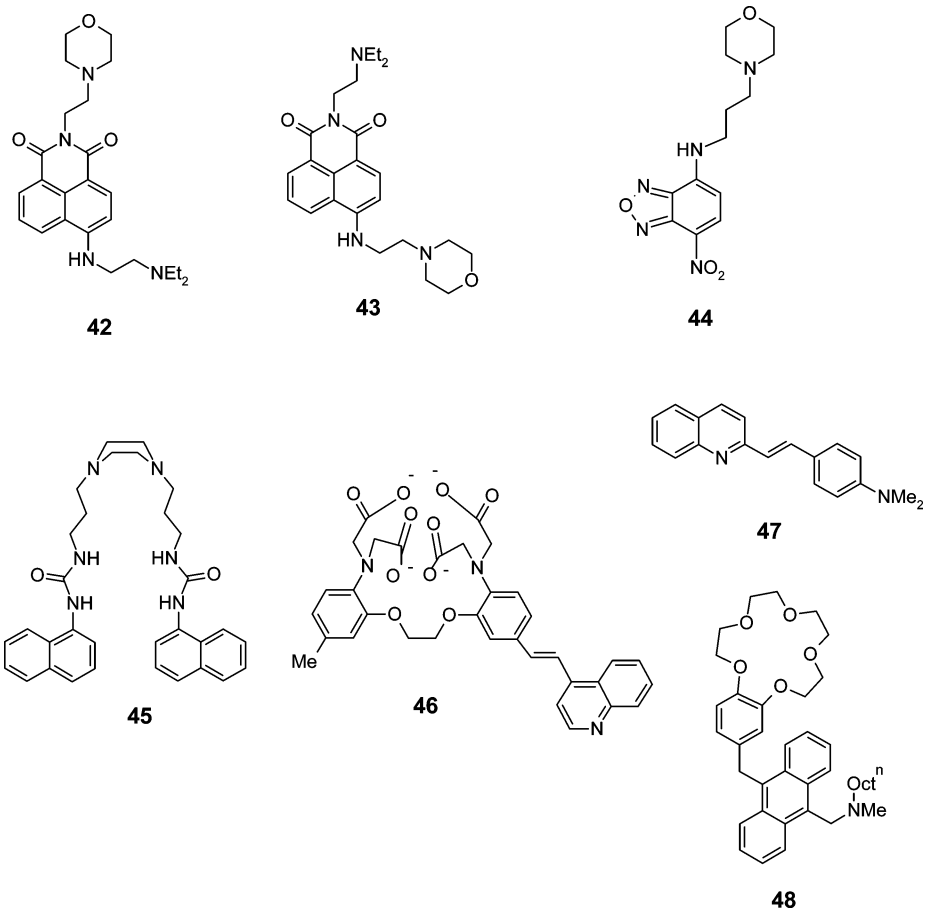

It is only fair to note that Wu and Mei's earlier example **45** has some conceptual similarity to **44** but differs in its purpose.[92] The integrated 'fluorophore–receptor' is a naphthylurea moiety. Hydrogen bonding occurs between the analyte, α,ω-dicarboxylate anions and the urea groups. Quenching of the fluorescence of the naphthalene group due to the hydrogen-bonding was observed, as well as the formation of a new emission at 500 nm arising from the anion–naphthylurea complex. The hydrogen bonding increases the amount of electron density on the naphthylurea, thus decreasing PET from the piperazine unit. This, in turn, causes an increase in fluorescence, as observed at 500 nm.

17. Cartoon 16: molecular XOR logic and arithmetic

Now, let's excise the remaining spacer in cartoon 15 and also focus on the light absorption aspect. Then we have integrated 'receptor–chromophore–receptor' systems. Our **46**[93] builds on the foundations of Wang and Ho's **47**.[94] Uniquely, **46** targets different analytes, H^+ and Ca^{2+}, *via* its two receptors. The energy of the ICT dipolar excited state is oppositely, and nearly equally, affected by H^+ and Ca^{2+} because of their arrival at the opposite ends of the chromophore. If we monitor the transmittance at the original absorption band maximum of **46**, we have a 'low' output. The H^+ and Ca^{2+} inputs are both 'low' in that state of **46**. If either input is 'high', the absorption band is displaced one way or the other, causing an increase of the transmittance output to the 'high' level. When both inputs are 'high', their effects on the absorption band virtually cancel. So the transmittance output remains 'low'. These four situations correspond to the truth table of XOR logic.[71] A nice older case of XOR logic is available from Balzani and Stoddart *et al*.[95] The parallel combination of an XOR logic gate with a suitable AND logic gate (cartoon 12), as commonly seen in semiconductor-based calculators and computers, allowed us to demonstrate molecular numeracy for the first time. The ability of molecules to conduct arithmetic operations has developed by a huge amount since then.[66–68]

18. Cartoon 17: molecular computation in nanospaces

The possibilities raised by practical molecular logic and computation outlined in cartoons 12 and 16 become interesting to non-chemists only if small space-scales with regard to semiconductor feature sizes can be demonstrated. Such a demonstration is possible in 3 nm spaces of detergent micelles.[96] A molecular AND logic gate can be persuaded to enter and operate in such spaces by following cartoon 17, where the AND gate of cartoon 12 is outfitted with a hydrophobic targeting module. Our **48** clearly displays AND logic in that 'high' fluorescence is seen only when the inputs H^+ and Na^+ are both 'high'.[97]

It is important to note that the entry of molecular logic gates into small spaces allows application straightaway (see Section 19), even though analogy with semiconductor devices would require more extensive solutions to the connectivity problem than those

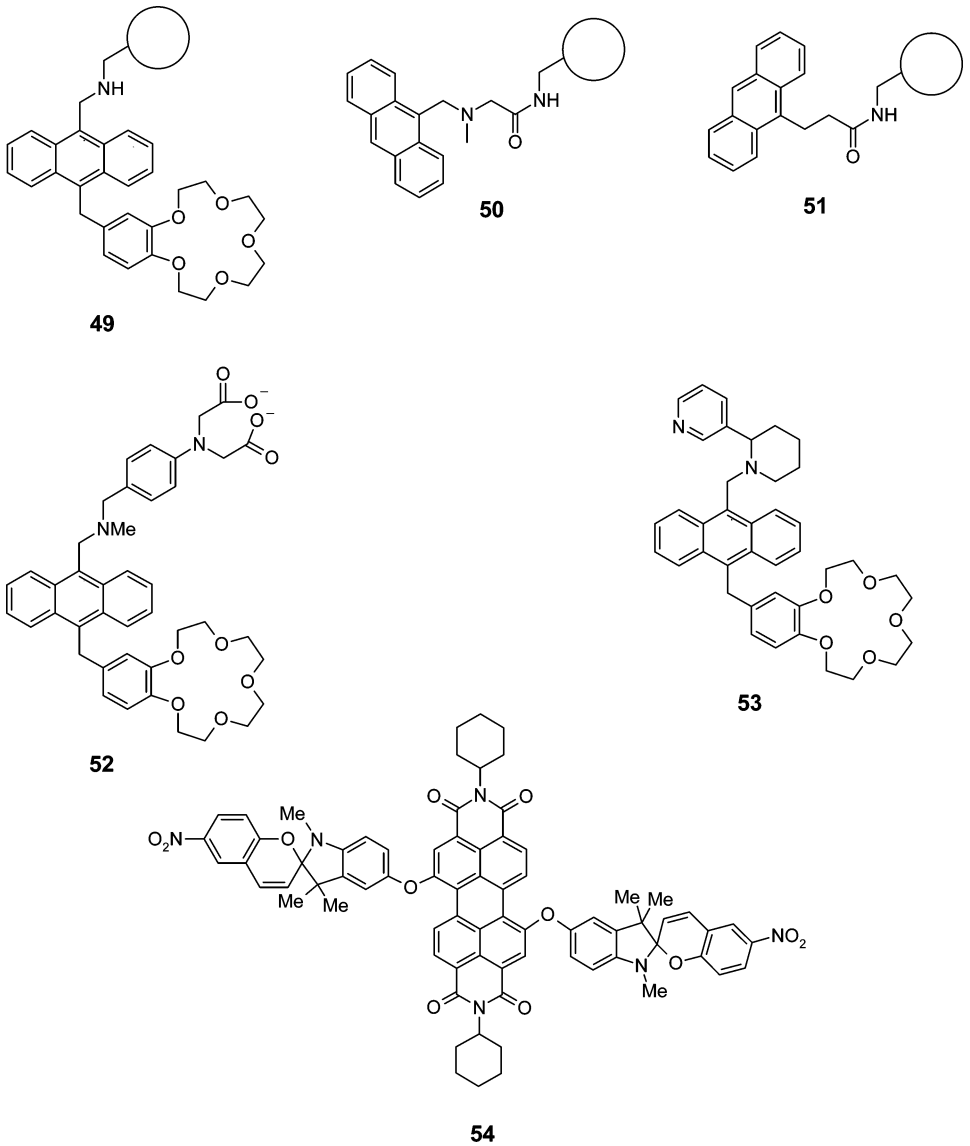

currently available.[40,65–68,74] It is now clear that developments in molecular logic and computation can diverge from semiconductor computer roadmaps and tackle different problems.[68]

19. Cartoon 18: molecular computational identification tags

Cartoon 18 can be grown from a permutation of cartoon 8 by adding another receptor and spacer, so that one of the applications mentioned under Section 9 can be developed further. Cartoon 18 (and permutations thereof) contains cartoon 12 within, and therefore brings the possibilities of molecular logic to the problem of identifying all small objects in large populations.[98] As mentioned in Section 9, the process of identification of an object consists of obtaining answers to a series of questions concerning its tag. A new question is 'what's the binary logic type of the tag?'. The answer could be any of the four single-input, single-output gates or any of the sixteen double-input, single-output gates etc.[71] For instance, **49** is a H^+, Na^+-driven AND logic gate tag on a polymer bead.[98] When the above question is considered together with the previous questions asked in Section 9, the number of distinguishable answers (and hence, identities) increases significantly. The parallel combination of logic gates allows a further sharp increase in diversity.

For instance, **50** and **51** are H^+-driven YES and PASS 1 logic gates respectively,[98] since the former switches 'on' its fluorescence only at low pH whereas the latter is fluorescent irrespective of pH. Indeed, **50** is similar to **22**[51] discussed in Section 9 whereas **51** is simply **50** after excision of its methylamino receptor unit. When a polymer bead is tagged with an equimolar mixture of **50** and **51**, a new fluorescence–pH profile emerges. Now the fluorescence intensity at low pH is only twice that when at high pH. This is hardly a binary 'on–off' switch, but well within the measurement capability of light detectors (within fluorescence spectrometers, for instance). Logic is not restricted to binary. However, multi-valued logic, *e.g.* ternary,[91] is not commonly found inside computers. The latter arises from the fact that ternary logic devices are less stable towards error accumulation,[99] *e.g.* 0, 1 and 2 start becoming indistinguishable at 50% error. This is not a limitation for our application since our errors are $<10\%$. Since multi-valued

logic is more information-rich than the binary variety, larger numbers of objects can potentially be individually identified by this extension of molecular computational identification (MCID). The application of MCID to a mixture of five different bead types is seen in a fluorescence micrograph (Fig. 4). As far as we are aware, MCID is the first application of molecular logic and computation that is not accessible to conventional semiconductor versions.

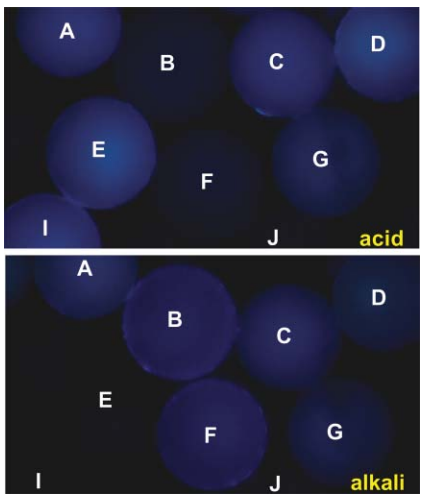

Fig. 4 Fluorescent micrographs demonstrating molecular computational identification (MCID) of 0.1 mm polymer beads. The beads are tagged with different logic gates and treated with acid (top panel) and then alkali (bottom panel) in aqueous methanol (1 : 1, v/v) under ultraviolet (366 nm) irradiation. The logic gate type of each bead is as follows: A; PASS 1, B; NOT, C; PASS 1, D; PASS 1 + YES (1 : 1), E; YES, F; NOT, G; PASS 1, I; YES, J; PASS 0 (photograph by David Coulson and Colin McCoy, School of Pharmacy, Queen's University of Belfast).

20. Cartoon 19: 'lab-on-a-molecule' systems

We have already seen the new areas exposed when we considered fluorescent systems carrying two receptors instead of just one. Can increasing the number of receptors up to three yield anything more in terms of ideas? Yes, indeed. The number three introduces the concept of a 'crowd'. So the expansion of cartoon 12 to cartoon 19 gives rise to 3-input AND logic gates, *e.g.* **52** where the fluorescence signal becomes 'high' only when a crowd of three chemical inputs are all 'high'.[100] Three PET processes are involved here, similar to those found in S. A. de Silva *et al.*'s Na^+-enabled, H^+-driven 'off–on–off' system **53**.[101] **52** can allow the rapid detection of disease states arising from the elevation of three electrolytes where, in effect, the clinical laboratory investigations and a preliminary diagnosis are made by this 'lab-on-a-molecule' **52**. A medical practitioner can subsequently separate the positives from the false positives by more examinations. Zhu *et al.*'s **54** is an older AND gate that responds to two chemical binding acts and one photochemical act.[102]

21. Conclusions

Cartoons continue to aid the growth of several areas of photoscience.[103] Our experience, as sketched above, is a contribution to this endeavour. It has led us to fluorescent, phosphorescent and f-f luminescent sensors, medical diagnostics and molecular computational elements. The future of photochemically functional molecules is clearly bright, and the participation of fresh minds will only make it brighter.

Acknowledgements

It is a great pleasure to acknowledge the vital contributions of Saman Sandanayake, Richard Bissell, Nimal Gunaratne, Mark Lynch, Glenn Maguire, Colin McCoy, Thorri Gunnlaugsson, Terry Rice, Pamela Maxwell, Isabelle Dixon, Jude Rademacher, Juliette Roiron, Nathan McClenaghan, Allen Huxley, Marc Schroeder, David Fox, Tom Moody, Gareth McClean, Sheenagh Weir, Gareth Brown, Sara Pagliari, Manel Querol, Bernadine McKinney, Bridgeen McCaughan, Seiichi Uchiyama, David Farrell, John Callan and David Magri to the research outlined here. Also, the support of DEL, EPSRC, EC, McClay Trust, Procter and Gamble Company, Japan Society for the Promotion of Science and Roche-AVL is much appreciated. We also acknowledge the collaborations with Jean-Philippe Soumillion, Jean-Louis Habib-Jiwan, Otto Wolfbeis, Jim Tusa, Hua-rui He, Marc Leiner and Kaoru Iwai as well as the guidance of Errol Fernando, Vincent Arkley, James and Jadwiga Grimshaw, and Ron Grigg.

References

1 R. A. Bissell, A. P. de Silva, H. Q. N. Gunaratne, P. L. M. Lynch, G. E. M. Maguire and K. R. A. S. Sandanayake, *Chem. Soc. Rev.*, 1992, **21**, 187.
2 A. P. de Silva and K. R. A. S. Sandanayake, *J. Chem. Soc., Chem. Commun.*, 1989, 1183.
3 M. Montalti, A. Credi, L. Prodi and M. T. Gandolfi, *Handbook of Photochemistry*, CRC Press, Boca Raton, 3rd edn, 2006.
4 A. Weller, *Pure Appl. Chem.*, 1968, **16**, 115.
5 *Electron Transfer*, ed. V. Balzani, Wiley-VCH, Weinheim, 2003.
6 R. A. Bissell, A. P. de Silva, H. Q. N. Gunaratne, P. L. M. Lynch, G. E. M. Maguire, C. P. McCoy and K. R. A. S. Sandanayake, *Top. Curr. Chem.*, 1993, **168**, 223.
7 A. P. de Silva, H. Q. N. Gunaratne, T. Gunnlaugsson, A. J. M. Huxley, C. P. McCoy, J. T. Rademacher and T. E. Rice, *Chem. Rev.*, 1997, **97**, 1515.
8 H. F. Ji, R. Dabestani, G. M. Brown and R. L. Hettich, *J. Chem. Soc., Perkin Trans. 2*, 2001, 585.
9 J. F. Callan, A. P. de Silva and D. C. Magri, *Tetrahedron*, 2005, **61**, 8551.
10 A. P. de Silva and R. A. D. D. Rupasinghe, *J. Chem. Soc., Chem. Commun.*, 1985, 1669.
11 R. P. Haugland, *The Handbook—A Guide to Fluorescent Probes and Labeling Technologies*, web edition: http://probes.invitrogen.com/handbook/.
12 S. Paglin, T. Hollister, T. Delohery, N. Hackett, M. McMahill, E. Sphicas, D. Domingo and J. Yahalom, *Cancer Res.*, 2001, **61**, 439.
13 R. Y. Tsien, *Am. J. Physiol.*, 1992, **263**, C723.
14 E. V. Anslyn, *J. Org. Chem.*, 2007, **72**, 687.
15 L. Fabbrizzi, F. Foti, M. Licchelli, A. Poggi, A. Taglietti and M. Vazquez, *Adv. Inorg. Chem.*, 2007, **59**, 81.
16 A. P. de Silva, S. S. K. de Silva, N. C. W. Goonesekera, H. Q. N. Gunaratne, P. L. M. Lynch, K. R. Nesbitt, S. T. Patuwathavithana and N. L. D. S. Ramyalal, *J. Am. Chem. Soc.*, 2007, **129**, 3050.
17 *Indicators*, ed. E. Bishop, Pergamon, Oxford, 1972.
18 R. A. Bissell, E. Calle, A. P. de Silva, S. A. de Silva, H. Q. N. Gunaratne, J. L. Habib-Jiwan, S. L. A. Peiris, R. A. D. D. Rupasinghe, T. K. S. D. Samarasinghe, K. R. A. S. Sandanayake and J.-P. Soumillion, *J. Chem. Soc., Perkin Trans. 2*, 1992, 1559.
19 J. F. Callan, A. P. de Silva, D. B. Fox, N. D. McClenaghan and K. R. A. S. Sandanayake, *J. Fluoresc.*, 2005, **15**, 769.
20 M. R. Wasielewski, in *Photoinduced Electron Transfer A*, ed. M. A. Fox and M. Chanon, Elsevier, Amsterdam, 1988, p. 161.

21 R. A. Bissell, A. P. de Silva, W. T. M. L. Fernando, S. T. Patuwathavithana and T. K. S. D. Samarasinghe, *Tetrahedron Lett.*, 1991, **32**, 425.
22 M. J. Hall, L. T. Allen and D. F. O'Shea, *Org. Biomol. Chem.*, 2006, **4**, 776.
23 C. J. Fahrni, L. C. Yang and D. G. VanDerveer, *J. Am. Chem. Soc.*, 2003, **125**, 3799.
24 F. Pragst and E. Weber, *J. Prakt. Chem./Chem.-Ztg.*, 1976, **318**, 51.
25 A. P. de Silva and H. Q. N. Gunaratne, *J. Chem. Soc., Chem. Commun.*, 1990, 186.
26 B. Valeur, *Molecular Fluorescence*, Wiley-VCH, Weinheim, 2001.
27 J. R. Lakowicz, *Principles of Fluorescence Spectroscopy*, Springer, 3rd edn, 2006.
28 H. Zollinger, *Color Chemistry*, VCH, Weinheim, 1991.
29 A. P. de Silva, H. Q. N. Gunaratne, J.-L. Habib-Jiwan, C. P. McCoy, T. E. Rice and J.-P. Soumillion, *Angew. Chem., Int. Ed. Engl.*, 1995, **34**, 1728.
30 Y. Q. Gao and R. A. Marcus, *J. Phys. Chem. A*, 2002, **106**, 1956.
31 A. P. de Silva, A. Goligher, H. Q. N. Gunaratne and T. E. Rice, *ARKIVOC*, 2003, **part vii**, 229.
32 A. P. de Silva, H. Q. N. Gunaratne and P. L. M. Lynch, *J. Chem. Soc., Perkin Trans. 2*, 1995, 685.
33 M. D. P. de Costa, A. P. de Silva and S. T. Pathirana, *Can. J. Chem.*, 1987, **69**, 1416.
34 D. W. Cui, X. H. Qian, F. Y. Liu and R. Zhang, *Org. Lett.*, 2004, **6**, 2757.
35 Y. Xiao, M. Y. Fu, X. H. Qian and J. N. Cui, *Tetrahedron Lett.*, 2005, **46**, 6289.
36 J. D. Bolt and N. J. Turro, *Photochem. Photobiol.*, 1982, **35**, 305.
37 N. J. C. Love and R. Weinberger, *Spectrochim. Acta, Part B*, 1983, **38**, 1421.
38 R. A. Bissell and A. P. de Silva, *J. Chem. Soc., Chem. Commun.*, 1991, 1148.
39 L. X. Mu, Y. Wang, Z. Zhang and W. J. Jin, *Chin. Chem. Lett.*, 2004, **15**, 1131.
40 A. P. de Silva, I. M. Dixon, H. Q. N. Gunaratne, T. Gunnlaugsson, P. R. S. Maxwell and T. E. Rice, *J. Am. Chem. Soc.*, 1999, **121**, 1393.
41 R. A. Beecroft, R. S. Davidson, D. Goodwin, J. E. Pratt and X. J. Luo, *J. Chem. Soc., Faraday Trans. 2*, 1986, **82**, 2393.
42 C. Hansch, A. Leo and D. Hoekman, *Exploring QSAR*, Oxford University Press, New York, 1995, vol. I and II.
43 R. A. Bissell, A. J. Bryan, A. P. de Silva and C. P. McCoy, *J. Chem. Soc., Chem. Commun.*, 1994, 405.
44 F. M. Harold, *The Vital Force: A Study of Bioenergetics*, Freeman, New York, 1986.
45 Y. Nakahara, T. Kida, Y. Nakatsuji and M. Akashi, *Chem. Commun.*, 2004, 224.
46 S. Uchiyama, K. Iwai and A. P. de Silva, *Angew. Chem., Int. Ed.*, 2008, **47**, in press.
47 H. A. Klok and M. Moller, *Macromol. Chem. Phys.*, 1996, **197**, 1395.
48 A. P. de Silva and S. A. de Silva, *J. Chem. Soc., Chem. Commun.*, 1986, 1709.
49 S. Buck, Y. E. L. Koo, E. Park, H. Xu, M. A. Philbert, M. A. Brasuel and R. Kopelman, *Curr. Opin. Chem. Biol.*, 2004, **8**, 540.
50 M. Ayadim, J.-L. Habib-Jiwan, A. P. de Silva and J.-P. Soumillion, *Tetrahedron Lett.*, 1996, **37**, 7039.
51 G. T. Copeland and S. J. Miller, *J. Am. Chem. Soc.*, 1999, **121**, 4306.
52 J. K. Tusa and H. He, *J. Mater. Chem.*, 2005, **15**, 2640.
53 www.optimedical.com.
54 A. P. de Silva, H. Q. N. Gunaratne, A. T. M. Kane and G. E. M. Maguire, *Chem. Lett.*, 1995, 125.
55 Z. Juan and T. M. Swager, *Adv. Polym. Sci.*, 2005, **177**, 151.
56 A. P. de Silva, H. Q. N. Gunaratne, T. Gunnlaugsson and P. L. M. Lynch, *New J. Chem.*, 1996, **20**, 871.
57 S. Banthia and A. Samanta, *J. Phys. Chem. B*, 2006, **110**, 6437.
58 A. Ojida, M. Mito-oka, K. Sada and I. Hamachi, *J. Am. Chem. Soc.*, 2004, **126**, 2454.
59 A. V. Koulov, K. A. Stucker, C. Lakshmi, J. P. Robinson and B. D. Smith, *Cell Death Differentiation*, 2003, **10**, 1357.
60 A. P. de Silva and K. R. A. S. Sandanayake, *Angew. Chem., Int. Ed. Engl.*, 1990, **29**, 1173.
61 *Comprehensive Coordination Chemistry II*, ed. J. A. McCleverty and T. J. Meyer, Springer/Elsevier, Berlin/Amsterdam, 2002.
62 E. V. Anslyn and D. O. Dougherty, *Modern Physical Organic Chemistry*, University Science Books, California, 2006.
63 F. Fages, J.-P. Desvergne, H. Bouas-Laurent, J.-M. Lehn, J. P. Konopelski, P. Marsau and Y. Barrans, *J. Chem. Soc., Chem. Commun.*, 1990, 655.
64 T. D. James, K. R. A. S. Sandanayake and S. Shinkai, *Angew. Chem., Int. Ed. Engl.*, 1994, **33**, 2207.
65 V. Balzani, M. Venturi and A. Credi, *Molecular Devices and Machines*, Wiley-VCH, Weinheim, 2003.
66 U. Pischel, *Angew. Chem., Int. Ed.*, 2007, **46**, 4026.
67 A. Credi, *Angew. Chem., Int. Ed.*, 2007, **46**, 5472.
68 A. P. de Silva and S. Uchiyama, *Nature Nanotechnol.*, 2007, **2**, 399.
69 A. P. de Silva, H. Q. N. Gunaratne and C. P. McCoy, *Nature*, 1993, **364**, 42.
70 G. Boole, *An Investigation of the Laws of Thought*, Dover, New York, 1958.
71 M. Ben-Ari, *Mathematical Logic for Computer Science*, Prentice-Hall, Hemel Hempstead, 1993.
72 B. Bag and P. K. Bharadwaj, *Chem. Commun.*, 2005, 513.
73 A. P. de Silva, S. A. de Silva, A. S. Dissanayake and K. R. A. S. Sandanayake, *J. Chem. Soc., Chem. Commun.*, 1989, 1054.
74 K. Szacilowski, *Chem.–Eur. J.*, 2004, **10**, 2520.
75 C. R. Cooper and T. D. James, *Chem. Commun.*, 1997, 1419.
76 A. P. de Silva, H. Q. N. Gunaratne, C. McVeigh, G. E. M. Maguire, P. R. S. Maxwell and E. O'Hanlon, *Chem. Commun.*, 1996, 2191.
77 A. P. de Silva, H. Q. N. Gunaratne and C. P. McCoy, *Chem. Commun.*, 1996, 2399.
78 S. A. de Silva, A. Zavaleta, D. E. Baron, O. Allam, E. V. Isidor, N. Kashimura and J. M. Percarpio, *Tetrahedron Lett.*, 1997, **38**, 2237.
79 R. Aucejo, J. Alarcon, E. Garcia-Espana, J. M. Llinares, K. L. Marchion, C. Soriano, C. Lodeiro, M. A. Bernardo, F. Pina, J. Pina and J. S. de Melo, *Eur. J. Inorg. Chem.*, 2005, 4301.
80 A. P. de Silva, H. Q. N. Gunaratne and T. E. Rice, *Angew. Chem., Int. Ed. Engl.*, 1996, **35**, 2116.
81 A. P. de Silva, H. Q. N. Gunaratne, T. E. Rice and S. Stewart, *Chem. Commun.*, 1997, 1891.
82 F. S. Richardson, *Chem. Rev.*, 1982, **82**, 541.
83 D. Parker, *Chem. Soc. Rev.*, 2004, **33**, 156.
84 T. Gunnlaugsson and J. P. Leonard, *Chem. Commun.*, 2005, 3114.
85 A. P. de Silva and T. E. Rice, *Chem. Commun.*, 1999, 163.
86 *The Photosynthetic Reaction Center*, ed. J. Deisenhofer and J. R. Norris, Academic Press, San Diego, 1993, vol. I and II.
87 M. R. Gunner, A. Nicholls and B. Honig, *J. Phys. Chem.*, 1996, **100**, 4277.
88 A. U. Acuna, *J. Chem. Educ.*, 2007, **84**, 231.
89 D. T Burns, B. G. Dalgarno, P. E. Gargan and J. Grimshaw, *Phytochemistry*, 1984, **23**, 167.
90 J. F. Callan, A. P. de Silva, J. Ferguson, A. J. M. Huxley and A. M. O'Brien, *Tetrahedron*, 2004, **60**, 11125.
91 B. Hayes, *Am. Scientist*, 2001, **89**, 490.
92 M. H. Mei and S. K. Wu, *New J. Chem.*, 2001, **25**, 471.
93 A. P. de Silva and N. D. McClenaghan, *J. Am. Chem. Soc.*, 2000, **122**, 3965.
94 S. L. Wang and T. I. Ho, *Chem. Phys. Lett.*, 1997, **268**, 434.
95 A. Credi, V. Balzani, S. J. Langford and J. F. Stoddart, *J. Am. Chem. Soc.*, 1997, **119**, 2679.
96 K. Sumaru, H. Matsuoka, H. Yamaoka and G. D. Wignall, *Phys. Rev. E*, 1996, **53**, 1744.
97 S. Uchiyama, G. D. McClean, K. Iwai and A. P. de Silva, *J. Am. Chem. Soc.*, 2005, **127**, 8920.
98 A. P. de Silva, M. R. James, B. O. F. McKinney, D. A. Pears and S. M. Weir, *Nat. Mater.*, 2006, **5**, 787.
99 R. W. Keyes, *Rev. Mod. Phys.*, 1989, **61**, 279.
100 D. C. Magri, G. J. Brown, G. D. McClean and A. P. de Silva, *J. Am. Chem. Soc.*, 2006, **128**, 4950.
101 S. A. de Silva, B. Amorelli, D. C. Isidor, K. C. Loo, K. E. Crooker and Y. E. Pena, *Chem. Commun.*, 2002, 1360.
102 X. Guo, D. Q. Zhang and D. B. Zhu, *Adv. Mater.*, 2004, **16**, 125.
103 V. Balzani, L. Moggi, and F. Scandola in *Supramolecular Photochemistry* , ed. V. Balzani, Reidel, Dordrecht, 1987, p. 1.

